

See discussions, stats, and author profiles for this publication at: <https://www.researchgate.net/publication/262637487>

# Influence of Subenvironmental Conditions and Thermodynamic Coupling on a Simple Reaction-Transport Process in Biochemical Systems

ARTICLE in INDUSTRIAL & ENGINEERING CHEMISTRY RESEARCH · APRIL 2014

Impact Factor: 2.59 · DOI: 10.1021/ie500941w

---

CITATIONS

3

READS

34

---

## 3 AUTHORS:



Rahul Tevadia

Vajra Instruments

8 PUBLICATIONS 20 CITATIONS

[SEE PROFILE](#)



Yasar Demirel

University of Nebraska at Lincoln

101 PUBLICATIONS 1,067 CITATIONS

[SEE PROFILE](#)



Paul Blum

University of Nebraska at Lincoln

81 PUBLICATIONS 2,453 CITATIONS

[SEE PROFILE](#)

# Influence of Subenvironmental Conditions and Thermodynamic Coupling on a Simple Reaction-Transport Process in Biochemical Systems

Rahul Tevadia,<sup>\*,†,‡</sup> Yaşar Demirel,<sup>†</sup> and Paul Blum<sup>‡</sup>

<sup>†</sup>Department of Chemical and Biomolecular Engineering, University of Nebraska Lincoln, Lincoln, Nebraska 68588, United States

<sup>‡</sup>Department of Biological Sciences, University of Nebraska Lincoln, Lincoln, Nebraska 68588, United States

 Supporting Information

**ABSTRACT:** Living systems must continuously receive substrates from subenvironment, and the population metabolic rate model is affected on this flow of substrates to be metabolized, its relevant variables, and the rate at which operates. This study focuses on the influences of resistances and bulk phase factors with in the subenvironment and by thermodynamic coupling on reaction-transport processes representing a simple enzymatic conversion of a substrate to a product. Thermodynamic coupling refers to mass flow, or a reaction velocity that occurs without or opposite to the direction imposed by its primary thermodynamic driving force. We considered the effects of (i) subenvironment resistances for the heat and mass flows of reacting substrate in the form of the ratios of Sherwood to Nusselt numbers, (ii) the subenvironment bulk phase temperatures and concentration of substrate, and (iii) the cross-coefficients responsible for the induced effects due to the thermodynamic coupling. In order to study these effects, the thermodynamically coupled balance equations using the first order simple elementary reaction are derived and solved numerically. In the balance equations, the linear phenomenological equations are used by assuming that the system is in the vicinity of global equilibrium. The overall results show that the subenvironment factors and cross-coefficients due to thermodynamic coupling may have considerable effects on reaction-transport processes.

## 1. INTRODUCTION

In order to maintain the self-organization and low-entropy structure processes, living systems must continuously receive nutrients from subenvironment. The population metabolic rate model focuses on this flow of nutrients to be metabolized, its relevant variables, and the rate at which operates.<sup>1–14</sup> The metabolism takes place due to the combined effects of many functional, synchronized, and thermodynamically coupled transport and rate processes within the system as a whole. Coupled reaction-transport processes are of great importance in biological systems; many biosynthesis processes, such as synthesis of the complex enzyme macromolecules from the amino acids, are nonspontaneous processes made possible by virtue of being coupled with other spontaneous processes such as oxidation of glucose.<sup>14</sup> Thermodynamic coupling refers to heat or mass flow, or a reaction velocity that occurs without or opposite to the direction imposed by its primary thermodynamic driving force as long as the cross-coefficients do not vanish. This is consistent with the statement of the second law, which states that a finite amount of organization may be purchased at the expense of a greater amount of disorganization in a series of coupled processes.<sup>6</sup> Some of the coupled processes in living systems include enzymatic reactions, thermal diffusivity in tissues, drug delivery, protein folding, biological oscillations, membrane transport, and the Turing instabilities with appropriate kinetics and large differences in diffusion rates<sup>7,15–18</sup> of metabolites.

One of the problems in bioenergetics is to understand the ability of complex coupled cycles of metabolism to achieve efficient and functional processes and their adaptation to

variable subenvironmental restrictions and topological factors.<sup>2–4,9,19</sup> A mathematical model<sup>3</sup> is used to analyze the transport of electron and proton thermodynamically coupled to adenosine triphosphate (ATP) synthesis in chloroplast by taking into account the nonuniform distribution of electron transport and ATP synthases complexes in the thylakoid of grana and stroma. For example, the rate of electron transfer at the plastoquinone site of the chain could be controlled not only by the intrathylakoid pH but also by the value of pH in the interthylakoid gap, which affects the rate of plastoquinone reduction.<sup>3</sup> Also, the rate of ATP synthesis depends on osmotic properties of a chloroplast incubation medium and hence on topological conditions. Turing pattern formation in two-layer coupled reaction-diffusion system is also affected by subenvironment and external influences to transport of substrates. Therefore, bilayer membranes or multilayer tissues under different subenvironments influences could affect the transport processes and hence pattern formation in complex thermodynamically coupled biological systems.<sup>4,7</sup>

A comprehensive approach toward understanding reaction-transport processes influenced by thermodynamic coupling, and subenvironment factors and resistances would be a valuable tool toward describing and formulating complex biochemical systems. Based on linear nonequilibrium thermodynamics approach,<sup>5,6,8,11,19–23</sup> this study presents a thorough analysis

**Received:** March 5, 2014

**Revised:** April 7, 2014

**Accepted:** April 9, 2014

**Published:** April 9, 2014



of thermodynamically coupled balance equations for the reaction-transport processes to illustrate the evolution of mass concentrations and temperatures of the substrate in time and space under the following influences: (i) the subenvironmental resistances to the heat and mass flows of substrates in the form of the ratios of Sherwood number to Nusselt number ( $Sh/Nu$ ) for a set of bulk phase conditions and cross-coefficients, (ii) the subenvironment bulk phase concentration and temperatures of the substrates for a set of the ratios of  $Sh/Nu$  and cross-coefficients, (iii) the cross-coefficients for a set of ratios of  $Sh/Nu$  and subenvironment bulk phase temperatures and concentrates.

## 2. REACTION-TRANSPORT PROCESSES WITHOUT THERMODYNAMIC COUPLING

The following simple elementary reaction



is considered and may represent simple reaction enzymatic reactions between a substrate and a product, unimolecular isomerization, or racemization of molecules with mirror-image structures with the forward and backward reactions rate constants of  $k_f$  and  $k_b$ , respectively.

The well-known balance equations for transport processes with the reaction considered in eq 1 are

$$\frac{\partial C_S}{\partial t} = -\nabla \cdot J_S + \nu_S J_r \quad (2)$$

$$\frac{\partial C_P}{\partial t} = -\nabla \cdot J_P + \nu_P J_r \quad (3)$$

$$\rho c_p \frac{\partial T}{\partial t} = -\nabla \cdot J_q + (-\Delta H_r) J_r \quad (4)$$

where  $\Delta H_r$  is the heat of reaction,  $\nu_i$  is the stoichiometric coefficient, which is negative for reactants,  $c_p$  and  $\rho$  are the heat capacity and density, respectively. By using the Fick and Fourier laws in one-dimensional domain of  $y$ -direction, eqs 2 to 4 become

$$\frac{\partial C_S}{\partial t} = D_{Se} \frac{\partial^2 C_S}{\partial y^2} + \nu_S J_r \quad (5)$$

$$\frac{\partial C_P}{\partial t} = D_{Pe} \frac{\partial^2 C_P}{\partial y^2} + \nu_P J_r \quad (6)$$

$$\rho c_p \frac{\partial T}{\partial t} = k_e \frac{\partial^2 T}{\partial y^2} + (-\Delta H_r) J_r \quad (7)$$

where  $D_{ie}$  is the effective diffusivity for species  $i$ , and  $k_e$  the effective thermal conductivity. For simple slab geometry with the half thickness of  $L$ , the initial and boundary conditions are

$$\begin{aligned} t = 0, \quad C_S &= C_{S0}, \quad T = T_0 \\ y = \pm L, \quad C_S &= C_{Ss}, \quad C_P = C_{Ps} \\ y = 0, \quad \frac{\partial C_S}{\partial y} &= \frac{\partial T}{\partial y} = 0 \quad (\text{symmetry conditions}) \end{aligned} \quad (8)$$

where  $C_{Ss}$  and  $C_{Ps}$  are the concentrations at the surface of the film. At stationary state, eliminating the reaction terms from eqs 5 and 6, and integrating twice with the boundary conditions

given above, concentrations of the species are related to each other by  $\theta_P = a_1 + a_2(1 - \theta_S)$  where  $\theta_S = (C_S/C_{Ss})$ ,  $\theta_P = (C_P/KC_{Ss})$ ,  $a_1 = (C_{Ps}/KC_{Ss})$ ,  $a_2 = (D_{Se}/KD_{Pe})$ , and  $K$  is the chemical reaction equilibrium constant. The value of  $a_1$  determines the direction of reaction; the net reaction is toward the P if  $a_1 < 1$ . Also, By eliminating of the reaction terms from eqs 5 and 7 and integrating twice with the known boundary conditions, the temperature is related to the concentration by  $\phi = 1 + \beta(1 - \theta_S)$  where  $\phi = (T/T_s)$ ,  $\beta = ((-\Delta H_r)D_{Se}C_{Ss}/(-\nu_S)k_e T_s)$ ; the value of  $\beta$  is a measure of nonisothermal effects; as  $\beta$  approaches zero, system becomes isothermal.<sup>5,24</sup>

## 3. REACTION-TRANSPORT PROCESSES WITH THERMODYNAMIC COUPLING

**3.1. Linear Nonequilibrium Thermodynamics.** The infinitesimal entropy change  $dS = d_e S + d_i S$  consists of the entropy flow ( $d_e S = -dS_{\text{surr}}$ ) into the system from the subenvironment and the internal rate of local entropy production  $d_i S/dt$ . The total local rate of entropy production is expressed by  $d_i S/dt = \sum J_i X_i$  where  $J_i$  and  $X_i$  are the conjugate flows and forces, respectively.<sup>2,5,6,8,13,25</sup> Linear phenomenological equations relate the flows to the forces  $J_i = \sum_k L_{ik} X_k$  where the  $L_{ik}$  represent the primary ( $i = k$ ) and the cross-coefficients ( $i \neq k$ ). These coefficients satisfy the various constraints, such as Onsager's reciprocity, Gibbs-Duhem equation at equilibrium, and the choice of reference frame for diffusivities. A necessary and sufficient condition for  $d_i S/dt \geq 0$  is that all its principal minors of the coefficients matrix  $[L]$  be non-negative  $L_{ii} > 0$  ( $i = 1, 2, \dots, n$ ) and  $L_{ii}L_{kk} > (1/4)(L_{ik} + L_{ki})^2$  for ( $i \neq k$ ;  $i, k = 1, 2, \dots, n$ ). Some of the coefficients  $L_{ik}$  may be identified using Fick's, Fourier's, and the mass action laws.

The reaction velocity  $J_r$  is mostly expressed as  $J_r = J_{rf}(1 - \exp(-A/RT))$ . If we expand this equation and consider the near global equilibrium state where the Gibbs free energy is less than 1.5 kJ/mol or  $|A/RT| \ll 1$ , then we may assume a linear relationship between the reaction velocity and the chemical affinity for an elementary reaction  $J_r = J_{rf} = L_{rr}A/T = J_{rf,eq}A/(RT)$  where  $L_{rr} = J_{rf,eq}/(RT)$  and depends on the rate constant and consequently on the equilibrium concentration  $C_{Seq}$  and the amount of chemical catalyst. Some biological pathways occur at near global equilibrium conditions. By the conservation of mass, some flow-force relations of the enzyme catalyzed and other chemical reactions can be described by a simple hyperbolic-tangent function.<sup>7,8,11-23,25</sup> Therefore, a plot of reaction velocity versus affinity has three regions; at regions with very high positive and negative affinity values with the reaction velocity is almost independent of affinity. In between these regions, the reaction velocity varies smoothly, leading to a quasi-linear region around the inflection point. This region extends the linear flow-force relations over 7 kJ/mol with a less than 15% error in the reaction velocity. This behavior is independent of the reaction rate constants and mainly occurs due to conservation conditions.<sup>26</sup> This may be justified due to the existence of multi-inflection points in specific enzymatic systems.<sup>19-23,26,27</sup>

The rate of entropy production for a simple one-dimensional heat conduction is  $d_i S/dt = -(J_q/T^2)(dT/dx) > 0$ , where  $J_q = -L_{qq}/T^2(dT/dx)$ , which is identical to Fourier's law of heat conduction with  $k = L_{qq}/T^2$ . The equation for  $J_q$  is valid when the relative variation of temperature is small within the mean free path distance  $\lambda$  in the case of gases  $(\lambda/T)(dT/dx) \ll 1$ . Since this condition is satisfied for most systems, the linear phenomenological equations are satisfactory approximations for

transport processes.<sup>5,6,22</sup> The LNET formulation does not require the mechanism of the thermodynamic coupling.<sup>5,6,8</sup>

**3.2. Local Rate of Entropy Production.** Local rate of entropy production for reaction-transport processes is<sup>5,8</sup>

$$\frac{dS}{dt} = J_q \cdot \nabla \left( \frac{1}{T} \right) - J_S \cdot \frac{(\nabla \mu_S)_{T,P}}{T} - J_P \cdot \frac{(\nabla \mu_P)_{T,P}}{T} + J_{rs} \frac{A}{T} \geq 0 \quad (9)$$

where  $(\nabla \mu_i)_{T,P} = \sum_{i=1}^{n-1} (\partial \mu_i / \partial C_i) \nabla C_i$ . By using the Gibbs–Duhem equation at constant temperature and pressure ( $C_S \nabla \mu_S + C_P \nabla \mu_P = 0$ ), and no volume flow condition ( $J_S V_S + J_P V_P = 0$ ), where  $V_i$  is the partial molar volume of species  $i$ , eq 9 becomes

$$\frac{dS}{dt} = -J_q \cdot \left( \frac{1}{T^2} \right) \nabla T - J_S \cdot \frac{1}{T} \lambda_S \nabla C_S + J_{rs} \frac{A}{T} \geq 0 \quad (10)$$

where  $\lambda_S = (1 + (C_S/C_P))(\partial \mu_S / \partial C_S)_{T,P}$  for ( $V_S \approx V_P$ ),  $J_i$  is the molar flow of species  $i$ ,  $\mu_i$  is the chemical potential of species  $i$ ,  $A$  is the affinity ( $A = -\sum v_i \mu_i$ ),  $J_r$  is the reaction velocity (rate) ( $dC_S/v_S dt = dC_P/v_P dt = J_r$ ), and  $J_q$  is the vector of reduced heat flow  $J_q = q - \sum_{i=1}^n j_i h_i$  where  $q$  is the total heat flow,  $h_i$  is the partial molar enthalpy of species  $i$ . Equation 10, excludes pressure, viscous, electrical, and magnetic effects; it consists of scalar processes of chemical reactions and vectorial processes of heat and mass flows.

**3.3. Linear Phenomenological Equations.** Equation 10 identifies the independent conjugate flows  $J_i$  and forces  $X_k$  to be used in the following linear phenomenological equations when the system is in the vicinity of global equilibrium.<sup>5,6,8,9,12,19–21</sup>

$$J_S = -L_{SS} \frac{1}{T} \lambda_S \nabla C_S - L_{Sq} \frac{1}{T^2} \nabla T + \mathbf{L}_{Sr} \frac{A}{T} \quad (11)$$

$$J_q = -L_{qs} \frac{1}{T} \lambda_S \nabla C_S - L_{qq} \frac{1}{T^2} \nabla T + \mathbf{L}_{qr} \frac{A}{T} \quad (12)$$

$$J_r = -\mathbf{L}_{rs} \cdot \frac{1}{T} \lambda_S \nabla C_S - \mathbf{L}_{rq} \cdot \frac{1}{T^2} \nabla T + L_{rr} \frac{A}{T} \quad (13)$$

Equations 11 to 13 represent the thermodynamically coupled reaction-transport processes where the flows are the function of all the forces present within the system. The coefficient matrix [ $L$ ] is symmetric and its elements obey the Onsager rule  $L_{ki} = L_{ik}$ . Equations 11 to 13 introduce cross-coefficients between heat and mass flows  $L_{sq} = L_{qs}$ , heat flow and chemical reaction velocity  $L_{qr} = L_{rq}$ , and mass flows and chemical reaction velocity  $L_{sr} = L_{rs}$ . These cross-coefficients can be related to the kinetic parameters and transport coefficients, and control the induced effects because of the thermodynamic coupling.<sup>6,8,18</sup>

The Curie–Prigogine principle states that “quantities whose tensorial characters differ by an odd number of ranks cannot interact in an isotropic medium.” Since the flows (fluxes) should have the same symmetry elements (symmetric under arbitrary space rotations and under space parities), a scalar flow, such as the rate of reaction, cannot be coupled with a vectorial flow of a transport process in an isotropic medium where an equilibrium-dividing surface is symmetric with respect to rotations around any local normal vector.<sup>5,13,14,19,22,23,25</sup> However, the symmetry properties alone are not sufficient for identifying physical coupling; the actual physics considered in deriving the entropy production equation and the specific structure, such as anisotropy, are necessary. Thus, in symmetrical membrane diffusional flows cannot be directly coupled to chemical reactions taking place in the membrane. However, in asymmetrical membrane such coupling may be possible.

**3.4. Phenomenological Coefficients.** Some processes will not be dependent on some of the forces when the appropriate cross-coefficients naturally vanish. For example, some degrees of imperfections due to parallel pathways of reaction or intrinsic uncoupling within the pathway itself may lead to leaks and slips in mitochondria. This, however, may add complexity to the phenomenological analysis, because failure of models to fit the properties of a system may be the result of, for example, unaccounted coupling.<sup>14,19,22</sup>

The diagonal elements of the phenomenological coefficients matrix  $\mathbf{L}$  may be identified using the Fick, Fourier, and the mass action laws. Comparison of the first term on the rhs of eq 11 with Fick's law ( $J = -D_{Se} \nabla C_S$ ) yields  $L_{SS} = D_{Se} T / \lambda_S$ . Similarly, comparison of the second term on the rhs of eq 12 with Fourier's law ( $J_q = -k_e \nabla T$ ) yields  $L_{qq} = k_e T^2$ . The cross-coefficients ( $L_{sq}$  or  $L_{qs}$ ) may be represented by the Soret coefficient ( $s_T$ )  $s_T = D_T / D_{Se}$ , or the thermal diffusion coefficient ( $D_T$ ), which are related to each other by  $L_{sq} = s_T D_{Se} T^2 C_S = D_T T^2 C_S$ . The  $L_{qs}$  ( $= D_T T^2 C_S$ ) may be expressed by the Dufour coefficient  $D_D$  by  $L_{qs} = D_D C_S T / \lambda_S$ . We may define two new effective diffusion coefficients of ( $D_{Te}$  and  $D_{De}$ ) that are related to the thermal diffusion and the Dufour effect, respectively  $D_{Te} = L_{sq} (1/T^2) = s_T D_{Se} C_S = D_T C_S$  and  $D_{De} = L_{qs} (\lambda_S / T) = D_D C_S$ . With these newly defined primary  $L_{ii}$  and cross-coefficients  $L_{ik}$  eqs 11 to 13 become

$$J_S = -D_{Se} \nabla C_S - D_{Te} \nabla T + \mathbf{L}_{Sr} \frac{A}{T} \quad (14)$$

$$J_q = -D_{De} \nabla C_S - k_e \nabla T + \mathbf{L}_{qr} \frac{A}{T} \quad (15)$$

$$J_r = -\mathbf{L}_{rs} \cdot \frac{1}{T} \lambda_S \nabla C_S - \mathbf{L}_{rq} \cdot \frac{1}{T^2} \nabla T + \frac{k_f C_{Seq}}{R} \frac{A}{T} \quad (16)$$

When we can control the temperature and concentration gradients, the coupling coefficients between the chemical reaction and the flows of mass and heat may be determined experimentally.<sup>5,8</sup> For a closed system at stationary state  $J_S = 0$ , and using  $A = RT \ln(J_{rf}/J_{rb})$  in eq 14, we get

$$\mathbf{L}_{Sr} = \frac{1}{R \ln(J_{rf}/J_{rb})} (D_{Se} \nabla C_S + D_{Te} \nabla T) = \mathbf{L}_{rs} \quad (17)$$

On the other hand, at chemical equilibrium, where  $A = 0$  and  $J_r = 0$ , we have

$$J_r = 0 = -\mathbf{L}_{rs} \cdot \frac{1}{T} \lambda_S \nabla C_S - \mathbf{L}_{rq} \cdot \frac{1}{T^2} \nabla T \quad (18)$$

and the two coupling coefficients are related to each other by  $\mathbf{L}_{rq} = -\mathbf{L}_{rs} T \lambda_S (\nabla C_S / \nabla T) = \mathbf{L}_{qr}$ . By using the relationship  $-C_{SS} s_T = \nabla C_S / \nabla T$  at steady state, the coefficient  $L_{rq}$  in terms of the Soret coefficient  $s_T$  becomes  $L_{rq} = L_{rs} T \lambda_S C_{SS} s_T$ , and we get

$$\mathbf{L}_{rq} = \frac{T \lambda_S C_{SS} s_T}{(A/T)} [D_{Se} \nabla C_S + D_{Te} \nabla T] = \mathbf{L}_{qr} \quad (19)$$

Equations 17 and 19 suggest that the cross-coefficients  $L_{rq}$  and  $L_{rs}$  are related to the gradients of concentration and temperature, and control the induced effects between vectorial flows of heat and mass, and the scalar reaction velocity in an anisotropic medium.

The coefficients help determine the degree of coupling between a pair of flows; the degree of coupling between the unidirectional heat and mass flows  $q_{sq}$  and between the

chemical reaction and the unidirectional heat and mass flows,  $q_{\text{Sr}}$  and  $q_{\text{rq}}$  are<sup>5,19,28</sup>

$$\begin{aligned} q_{\text{Sq}} &= \frac{L_{\text{Sq}}}{(L_{\text{SS}} L_{\text{qq}})^{1/2}}, & q_{\text{Sr}} &= \frac{L_{\text{Sr}}}{(L_{\text{SS}} L_{\text{rr}})^{1/2}}, \\ q_{\text{rq}} &= \frac{L_{\text{rq}}}{(L_{\text{rr}} L_{\text{qq}})^{1/2}} \end{aligned} \quad (20)$$

### 3.5. Thermodynamically Coupled Balance Equations.

By inserting eqs 14 to 16 into eq 4 and eq 6, we may describe the thermodynamically coupled system of chemical reaction and the flows of heat and mass by

$$\begin{aligned} \frac{\partial C_S}{\partial t} &= -\nabla \cdot \left( -D_{\text{Se}} \nabla C_S - D_{\text{Te}} \nabla T + \mathbf{L}_{\text{Sr}} \frac{A}{T} \right) \\ &\quad - \left( -\mathbf{L}_{\text{rs}} \frac{\lambda_S}{T} \nabla C_S - \frac{\mathbf{L}_{\text{rq}}}{T^2} \cdot \nabla T + \frac{k_f C_{\text{S,eq}}}{R} \frac{A}{T} \right) \end{aligned} \quad (21)$$

$$\begin{aligned} \rho c_p \frac{\partial T}{\partial t} &= -\nabla \cdot \left( -D_{\text{De}} \nabla C_S - k_e \nabla T + \mathbf{L}_{\text{qr}} \frac{A}{T} \right) \\ &\quad + (-\Delta H_r) \left( -\mathbf{L}_{\text{rs}} \frac{\lambda_S}{T} \nabla C_S - \frac{\mathbf{L}_{\text{rq}}}{T^2} \cdot \nabla T + \frac{k_f C_{\text{S,eq}}}{R} \frac{A}{T} \right) \end{aligned} \quad (22)$$

Under mechanical equilibrium, we have

$$\nabla \left( \frac{\mu_i}{T} \right) = -H_i \frac{\nabla T}{T^2} + \frac{(\nabla \mu_i)_T}{T} \quad (23)$$

where  $H_i$  is the partial enthalpy of species  $i$ . By using the definition of affinity ( $A = \mu_s - \mu_p$ ), the Gibbs–Duhem equation ( $C_S \nabla \mu_s + C_p \nabla \mu_p = 0$ ),  $\lambda_S = (1 + (C_S/C_p))(\partial \mu_s / \partial C_S)_{T,P}$  (for  $V_S = V_p$ ),  $\Delta G_r^\circ + T \Delta S_r = \Delta H_r$ , and eq 23, we obtain

$$\nabla \left( \frac{A}{T} \right) = \left( \nabla \left( \frac{\mu_s}{T} \right) - \nabla \left( \frac{\mu_p}{T} \right) \right) = \frac{\lambda_S}{T} \nabla C_S - \frac{(-\Delta H_r)}{T^2} \nabla T \quad (24)$$

Substituting eq 24 in eqs 21 and 22, we have

$$\frac{\partial C_S}{\partial t} = D_{\text{Se}} \nabla^2 C_S + D_{\text{Te}} \nabla^2 T + \left( \frac{\mathbf{L}_{\text{rq}} + \mathbf{L}_{\text{Sr}}(-\Delta H_r)}{T^2} \right) \cdot \nabla T - I \quad (25)$$

$$\begin{aligned} \rho c_p \frac{\partial T}{\partial t} &= D_{\text{De}} \nabla^2 C_S + k_e \nabla^2 T - \left( \frac{\lambda_S [(-\Delta H_r) \mathbf{L}_{\text{rs}} + \mathbf{L}_{\text{qr}}]}{T} \right) \\ &\quad \cdot \nabla C_S + (-\Delta H_r) I \end{aligned} \quad (26)$$

where

$$I = \left[ C_{\text{S,eq}} k_o \exp \left( \frac{-E_f}{RT} \right) \right] \left( \frac{E_b - E_f}{RT} + \ln \left( \frac{C_s}{C_p} \right) \right)$$

$(A/RT) = \ln k(T) + \ln((a_s/a_p)) = \ln(k_f/k_b) + \ln(C_s/C_p)$  where the activities of species are assumed to be equal to concentrations  $C_s$  and  $C_p$ , respectively, by neglecting the nonideality effects on the species. Using the Arrhenius equations, we have  $\ln(k_f/k_b) = (E_b - E_f)/RT$ .

One-dimensional forms of eqs 25 and 26 in the  $y$ -direction are

$$\frac{\partial C_S}{\partial t} = D_{\text{Se}} \frac{\partial^2 C_S}{\partial y^2} + D_{\text{Te}} \frac{\partial^2 T}{\partial y^2} + \frac{b}{T^2} \frac{\partial T}{\partial y} - I \quad (27)$$

$$\frac{\partial T}{\partial t} = \frac{D_{\text{De}}}{\rho c_p} \frac{\partial^2 C_S}{\partial y^2} + \alpha_e \frac{\partial^2 T}{\partial y^2} - \frac{\lambda_S b}{\rho c_p T} \frac{\partial C_S}{\partial y} + \frac{(-\Delta H_r)}{\rho c_p} I \quad (28)$$

where  $b = L_{\text{rq}} + L_{\text{Sr}}(-\Delta H_r) = ((k_f C_{\text{S,eq}} T) / R)(k_e T q_{\text{rq}}^2 + (D_{\text{Se}}/\lambda_S) q_{\text{rq}}^2 (-\Delta H_r))$ ,  $q_{\text{rq}}$  and  $q_{\text{Sr}}$  are the degrees of coupling between reaction and heat flow and reaction and mass flow, respectively. Equations 27 and 28 use the initial and boundary conditions, which reflect the subenvironmental conditions

$$\begin{aligned} t = 0, \quad C_S &= C_{\text{So}}, \quad T = T_0 \\ y = \pm L, \quad \frac{\partial C_S}{\partial y} &= \frac{k_{\text{gS}}}{D_S} (C_{\text{Sb}} - C_{\text{Ss}}), \\ \frac{\partial T}{\partial y} &= \frac{h_f}{k} (T_b - T_s) \\ y = 0, \quad \frac{\partial C_S}{\partial y} &= \frac{\partial T}{\partial y} = 0 \quad (\text{symmetry conditions}) \end{aligned} \quad (29)$$

Nondimensional forms of eqs 27 and 28 become

$$\begin{aligned} \frac{\partial \theta_S}{\partial \tau} &= \frac{\partial^2 \theta_S}{\partial z^2} + \varepsilon \frac{\partial^2 \phi}{\partial z^2} + \frac{\sigma}{\phi^2} \frac{\partial \phi}{\partial z} \\ &\quad - A^* \text{Da}_S \theta_{\text{S,eq}} \exp \left[ \gamma_f \left( 1 - \frac{1}{\phi} \right) \right] \end{aligned} \quad (30)$$

$$\begin{aligned} \frac{1}{\text{Le}} \frac{\partial \phi}{\partial \tau} &= \frac{\partial^2 \phi}{\partial z^2} + \omega \frac{\partial^2 \theta_S}{\partial z^2} - \frac{\kappa}{\phi} \frac{\partial \theta_S}{\partial z} + A^* \text{Da}_S \beta \\ \theta_{\text{S,eq}} \exp \left[ \gamma_f \left( 1 - \frac{1}{\phi} \right) \right] \end{aligned} \quad (31)$$

where

$$\begin{aligned} z &= \frac{y}{L}, \quad \tau = \frac{D_{\text{Se}} t}{L^2}, \quad \text{Da}_S = \frac{L^2 k_o \exp(E_f/RT_s)}{D_{\text{Se}}}, \\ \gamma_f &= \frac{E_f}{RT_s}, \quad \gamma_b = \frac{E_b}{RT_s}, \quad \text{Le} = \frac{k_e / \rho C_p}{D_{\text{S,e}}} = \frac{\alpha_e}{D_{\text{S,e}}} \\ \varepsilon &= \frac{D_{\text{Te}} T_s}{D_{\text{Se}} C_{\text{Ss}}}, \quad \omega = \frac{D_{\text{De}} \epsilon_s}{k_e T_s}, \\ \sigma &= \frac{b L}{T_s D_{\text{Se}} C_{\text{Ss}}} = \frac{[L_{\text{rq}} + L_{\text{Sr}}(-\Delta H_r)] L}{T_s D_{\text{Se}} C_{\text{Ss}}}, \\ \kappa &= \frac{b C_{\text{Ss}} L \lambda_S}{k_e T_s^2} \end{aligned}$$

and

$$A^* = \left( \frac{\gamma_b - \gamma_f}{\phi} \right) + \ln \left( \frac{\theta_s}{K[a_1 + a_2(1 - \theta_s)]} \right)$$

$\text{Da}_i$  is the Damköhler number for component  $i$ , and measures the intrinsic rates of the reaction relative to that of the diffusions.

Equations 30 and 31 suggest that the induced effects due to the coupling phenomena and subenvironmental effects can increase the possibility that the system may evolve to multiple

states and diversify its behavior.<sup>13,22</sup> The parameters  $\varepsilon$ ,  $\sigma$ ,  $\omega$ , and  $\kappa$  above are associated with the cross-coefficients and hence control the coupled phenomena in the  $y$ -direction. Specifically, the  $\varepsilon$  and  $\omega$  control the coupling between mass and heat flows, while the  $\sigma$  and  $\kappa$  control the coupling between the chemical reaction and mass flow, and chemical reaction and heat flow, respectively.

The nondimensional forms of initial and boundary conditions described in eq 29 become

$$\begin{aligned} \tau = 0 \quad \theta_S &= \theta_{S_0}, \quad \phi = \phi_0 \\ z = \pm 1, \quad \tau > 0 \quad \frac{\partial \theta_S}{\partial z} &= Sh_S(\theta_{Sb} - 1), \quad \frac{\partial \phi}{\partial z} = Nu(\phi_b - 1) \\ z = 0, \quad \tau > 0 \quad \frac{\partial \theta_S}{\partial z} &= \frac{\partial \phi}{\partial z} = 0 \end{aligned} \quad (32)$$

where the Sh and Nu are the Sherwood and Nusselt numbers,  $Sh/Nu = (k_g L/D_s)/(h L/k_e)$  respectively. The dimensionless subenvironmental bulk phase concentrations of S is denoted by  $\theta_{Sb}$  and whereas  $\phi_b$  is the dimensionless subenvironmental bulk phase temperature. Accuracy of the solutions obtained from eqs 30 and 31 depends on the reliable data, such as the effective transport coefficients and cross-coefficients. Some processes will not be dependent on some of the forces when some of the cross-coefficients vanish naturally. For example, some degrees of imperfections due to parallel pathways of reaction or intrinsic uncoupling within the pathway itself may lead to leaks and slips in mitochondria.<sup>3,5</sup>

The balance equations of 5 and 7 can be combined at steady state as follows

$$\frac{d^2}{dy^2} \left( D_e C_S + \frac{k_e T}{(-\Delta H_r)} \right) = 0 \quad (33)$$

and integrated twice from the center to the surface using the boundary conditions addressing the subenvironmental conditions given in eq 29. The integration yields the following sum of external and internal temperature differences

$$T - T_b = (-\Delta H_r) \frac{k_g}{h} (C_b - C_{Ss}) + (-\Delta H_r) \frac{D_e}{k_e} (C_{Ss} - C_S) \quad (34)$$

The maximum temperature difference occurs when all the substrate is consumed ( $C_S = 0$ ), and after rearranging the terms, the effect of the ratio ( $Sh/Nu$ ) on the subenvironmental conditions are obtained

$$\frac{(T - T_b)_{max}}{T_b} = \beta_b \left[ \frac{Sh}{Nu} \left( 1 - \frac{C_{Ss}}{C_b} \right) + \frac{C_{Ss}}{C_b} \right] \quad (35)$$

## 4. RESULTS AND DISCUSSION

Nondimensional forms of eqs 30–31 representing the one-dimensional thermodynamically coupled reaction-transport processes are solved numerically using MATLAB with initial and boundary conditions given in eq 32 to determine the changes of  $\theta_S$  and  $\phi$  in space and time. To illustrate the subenvironmental influences and of the thermodynamic coupling on the reaction-transport systems, we considered the following:

- (i) Subenvironment resistances to the heat and mass flows of the substrates in the form of the ratios of Sherwood to

Nusselt numbers ( $Sh/Nu$ ) for a set of subenvironment bulk phase conditions and cross-coefficients shown in Table 1.

**Table 1. Parameters Used for the Reaction-Transport Processes**

param.	Figure 1	Figure 2	Figure 3
$\beta$	0.1	0.1	0.1
$\gamma$	10	10	10
Le	0.01	0.01	0.01
$Da_S$	0.01	0.01	0.01
$\delta$	1.0	1.0	1.0
$(Sh/Nu)_L$	<b>0.1<sup>a</sup></b>	n.u. <sup>b</sup>	n.u.
$(Sh/Nu)_H$	<b>20</b>	20	20
$(\theta_{Sb})_L$ <sup>c</sup>	0.9	<b>0.9</b>	0.9
$(\theta_{Sb})_H$ <sup>d</sup>	n.u.	<b>1.02</b>	n.u.
$(\phi_b)_L$	n.u.	<b>0.9</b>	n.u.
$(\phi_b)_H$	1.02	<b>1.02</b>	1.02
$(\varepsilon)_L$	0.0001	0.0001	<b>0.0001</b>
$(\varepsilon)_H$	n.u.	n.u.	<b>0.9</b>
$(\omega)_L$	0.0001	0.0001	<b>0.0001</b>
$(\omega)_H$	n.u.	n.u.	<b>0.9</b>
$(\sigma)_L$	0.0001	0.0001	<b>0.0001</b>
$(\sigma)_H$	n.u.	n.u.	<b>0.9</b>
$(\kappa)_L$	0.0001	0.0001	<b>0.0001</b>
$(\kappa)_H$	n.u.	n.u.	<b>0.9</b>

<sup>a</sup>Boldface parameters are used for comparison, while keeping other parameters constant. <sup>b</sup>n.u.: not used. <sup>c</sup>L: lower value. <sup>d</sup>H: higher value.

- (ii) Subenvironment bulk phase concentration and temperatures of the substrates for a set of the ratios of  $Sh/Nu$  and cross-coefficients shown in Table 1.
- (iii) Cross-coefficients for a set of the ratios of  $Sh/Nu$  and subenvironment bulk phase conditions for substrates, as shown in Table 1.

The values of parameters and coefficients used in this study are in line with the previously established limits.<sup>5,9,10,24,29,30</sup> The solutions are for slow chemical first order reactions ( $Da_S = 0.01$ ). The nondimensional group  $\beta$  (thermicity), which is the ratio of heat generation due to the reaction and rate of heat conduction, is kept constant at a value of 0.1. The Arrhenius ( $\gamma$ ) and Lewis numbers (Le) are kept constant during the study.

**4.1. Influences of Subenvironment Resistances to Heat and Mass Flows.** The ratio of  $Sh/Nu$  is largely dependent on the rates of heat and mass flows in subenvironment,<sup>10,30</sup> and may be one of the controlling parameters for mass and/or heat transfer limited chemical systems, such as DNA–protein and DNA–RNA interactions.<sup>5,9,17–21</sup> The considered low and high values for the ratio of  $Sh/Nu$  are 0.1 and 20, respectively, to represent the effects of subenvironment resistances to heat and mass flows (see Table 1 for the values of other parameters). Figure 1 displays the surface plots of changes for  $\theta_S$  and  $\phi$  with time and space at high and low ratios of  $Sh/Nu$ . Supporting Information Figure S1 shows the two-dimensional plots representing the effects of subenvironment resistances to the heat and mass flows of the substrates in the form of the ratios of Sherwood to Nusselt numbers ( $Sh/Nu$ ) with space ( $\tau = 1$ ) and time ( $z = 1$ ) for a set of subenvironment bulk phase conditions and cross-coefficients shown in Table S1, Supporting Information. The ratio  $Sh/Nu$  of 20 shows greater end effects on the surface of  $\theta_S$  than the

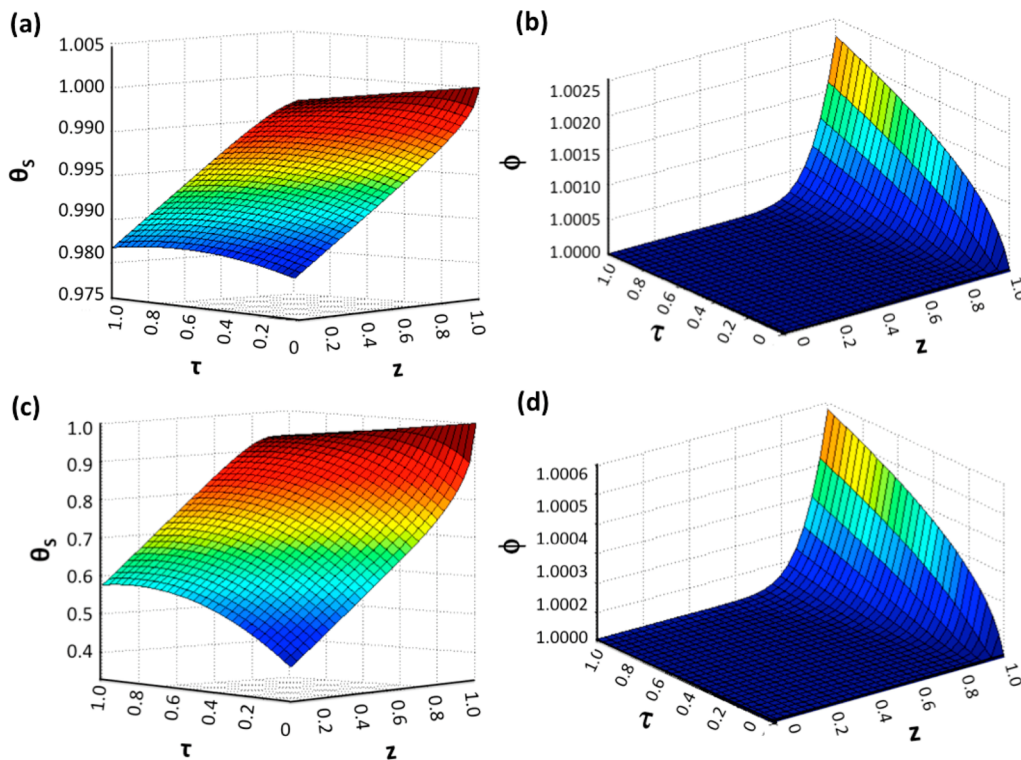


**Figure 1.** Surface plots showing the changes in  $\theta_s$  and  $\phi$  for coupled reaction-transport system with subenvironmental resistance in time and space keeping other parameters constant listed in Table 1: (a and b) Sh/Nu = 0.1; (c and d) Sh/Nu = 20.

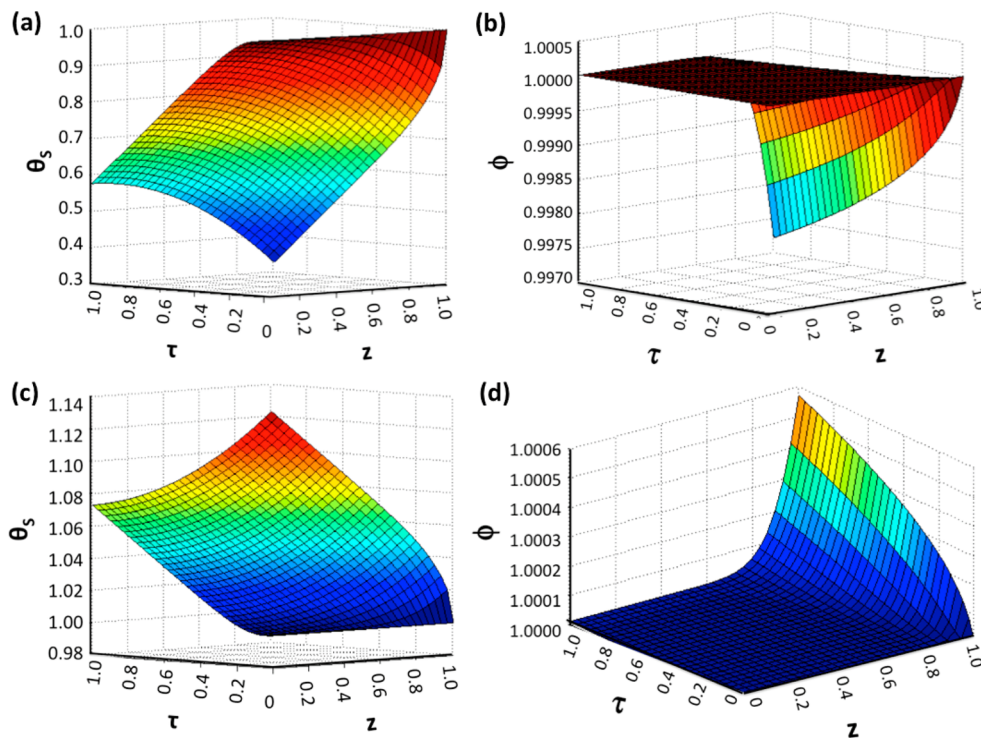


**Figure 2.** Surface plots showing changes  $\theta_s$  and  $\phi$  with subenvironmental bulk substrate concentration and temperature in time and space keeping other parameters constant listed in Table 1: (a and b)  $\theta_{sb} < 1$ ,  $\phi_b < 1$ ; (c and d)  $\theta_{sb} > 1$ ,  $\phi_b > 1$ .

effects due to Sh/Nu of 0.1 (Figure 1a and c). When the ratio Sh/Nu = 20, the  $\theta_s$  decreases considerably while  $\phi$  increases only slightly in both time and space, indicating little resistance for the mass flow form bulk to the surface and eventually to the reacting site (Figure 1c). On other hand, if the ratio is less than

one (Sh/Nu = 0.1), the heat flow is faster and lower rate of mass flows lead to the small decrease in  $\theta_s$  while considerable increase in  $\phi$  in both time and space (Figure 1a). The end effects are also noticeable in Figure 1b, where  $\phi$  increases to 1.0025, while at Sh/Nu = 0.1  $\phi$  increases to 1.0006 (Figure 1d).

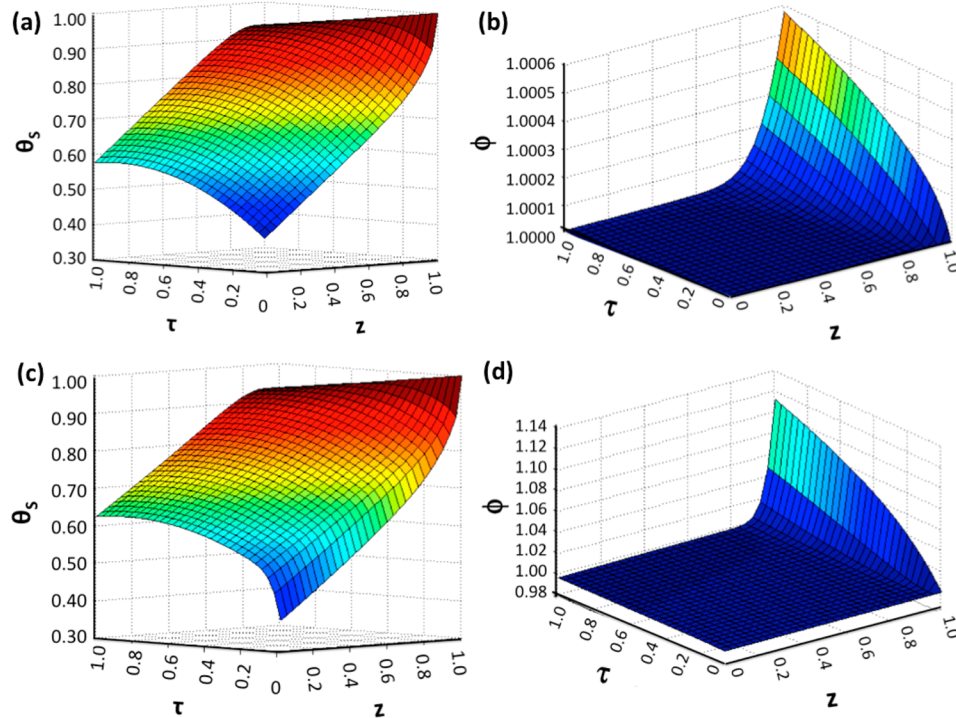


**Figure 3.** Surface plots showing changes in  $\theta_s$  and  $\phi$  with reaction-heat, reaction-mass, and heat-mass flows cross-coefficients in time and space keeping other parameters constant listed in Table 1: (a and b)  $\sigma = 0.0001$ ,  $\kappa = 0.0001$ ,  $\varepsilon = 0.0001$ ,  $\omega = 0.0001$ ; (c and d)  $\sigma = 0.9$ ,  $\kappa = 0.9$ ,  $\varepsilon = 0.9$ ,  $\omega = 0.9$ .

As Figure 1, parts b and d, shows, temperature changes are quite visible at when  $Nu > Sh$ . Figure 1d indicates a sharp change of temperature toward the end of space region of around  $z = 0.7$ . Therefore, if the mass flow is slower, such as reactants are in gaseous phase and the enzyme is in the solid phase, the heat flow becomes an important factor to the overall reaction.

#### 4.2. Influences of Subenvironment Bulk Phase Conditions.

The bulk concentration and bulk temperature can affect various biochemical events and biological processes.<sup>5</sup> For example, the nitrogen source concentration (bulk concentration) can influence the microalgal growth and neutral lipid production.<sup>10</sup> The bulk temperature also impacts transport processes<sup>5</sup> and protein folding<sup>17</sup> within the cell. The dimensionless values of bulk concentrations and bulk temperature considered are  $\theta_{sb} < 1$  and  $\phi_b < 1$  and  $\theta_{sb} > 1$  and  $\phi_b > 1$  (with other parameters listed in Table 1). Figure 2 shows surface plots of concentration and temperature illustrating an inverse behavior for the values of bulk concentration as well as temperature for higher and lower values than one. Supporting Information Figure S2 shows two-dimensional plots indicating the effects of subenvironment bulk phase concentration and bulk temperatures on  $\theta_s$  and  $\phi$  with space ( $\tau = 1$ ) and time ( $z = 1$ ) for a set of the ratios of  $Sh/Nu$  and cross-coefficients shown in Table S1, Supporting Information. The substrate concentration consistently decreases with  $\theta_{sb} < 1$  and  $\phi_b < 1$  (Figure 2a) and increase uniformly with  $\theta_{sb} > 1$  and  $\phi_b > 1$  (Figure 2c). When  $\theta_{sb} > 1$  and  $\phi_b > 1$ , the change in substrate concentration remains almost constant with the value around 1.00–1.10 with space at  $\tau = 1$ , and 1.00–1.05 with time at  $z = 1$ . On other hand, when, the substrate concentration decreases rapidly from 1.00 to 0.30, and from 0.60 to 0.30 with  $\tau$  at  $z = 1$ . It is evident from the temperature profiles (Figure 2b and d) that the changes in temperature are mostly at  $z \geq 0.7$ . Therefore, a

slight increase in temperature can be observed for  $\theta_{sb} > 1$  and  $\phi_b > 1$ , and the decrease is quite rapid when  $\theta_{sb} < 1$  and  $\phi_b < 1$ , toward the end of space around  $z \geq 0.7$  can be detected. Consequently, in order to attain effective substrate conversion and temperature utilization, the bulk resistances must be low. Hence, impact of subenvironment bulk condition is one of the important factors that control the changes of concentration and temperature in reaction-transport processes.

#### 4.3. Influence of Thermodynamic Coupling.

Equations 30 and 31 are for thermodynamically coupled system of unidirectional reaction-transport processes with some unique cross-coefficients between the chemical reaction and heat and mass flow, and between mass and heat flows. The cross-coefficient  $\sigma$  controls the coupling between the chemical reaction velocity and mass flow,  $\kappa$  controls the coupling between the chemical reaction velocity and heat flow,  $\varepsilon$  controls the coupling between heat and mass flows involving Soret effect, and  $\omega$  controls the coupling between heat and mass flows involving Dufour effect on the thermodynamically coupled reaction-transport systems.<sup>5,8</sup> The solutions shown in Figure 3 are for low values (0.0001) and high values (0.9) for the cross-coefficients of  $\sigma$ ,  $\kappa$ ,  $\varepsilon$ , and  $\omega$ , while keeping the same subenvironment resistances and bulk conditions as shown in Table 1. Supporting Information Figure S3 shows two-dimensional plots summarizing the effects of cross-coefficients involved in coupling of reaction-heat flow, reaction-mass flow, and heat-mass flows on  $\theta_s$  and  $\phi$  with space ( $\tau = 1$ ) and time ( $z = 1$ ) for a set of the ratios of  $Sh/Nu$ , and bulk substrate concentration and temperature shown in Table S1, Supporting Information. The overall effects of thermodynamic coupling on substrate profile can be observed in the surface plots, where the conversion is relatively greater for high values of cross-coefficients (Figure 3). For both high and low values of the cross-coefficients,  $\theta_s$  reduces with time and space. The

**Table 2. Biological Significance of the Parameters Involved in Subenvironmental Factors and Coupling between Reaction Velocity, Mass Flow, and Heat Flow**

param.	definition	biological significance
(a) Subenvironment Resistances $Sh/Nu = (k_g L/D_s)/(h_i L/k_e)$	ratio of Sherwood to Nusselt number	The ratio shows the relative rate of the mass transport to heat transport. <sup>5,24,29</sup>
(b) Subenvironment Bulk Phase $\theta_{Sb} = (C_{Sb}/\theta_{Ss})$	bulk phase dimensionless substrate concentration	Bulk phase concentration and temperature has a significant impact over several biological modification and transport. <sup>5,10,17</sup> For instance, protein convective transport and adsorption depend on bulk phases conditions.
$\phi_b = (T_b/T_s)$	bulk phase dimensionless temperature	
(c) Cross-coefficients $\varepsilon = D_{Te}T/D_{Se}C_{Ss}$	$\varepsilon$ controls the coupling between heat and mass flows involving Soret effect	This cross-coefficients controls the induced mass fluxes that occur due to a temperature gradient without a corresponding concentration gradient. <sup>5,6,11</sup>
$\omega = D_{De}C_S/k_e T$	$\omega$ controls the coupling between heat and mass flows involving Dufour effect	This cross-coefficient controls the induced heat flux by chemical potential gradient of substrate without temperature gradient. <sup>3,5,6</sup>
$\sigma = [L_{rq} + L_{sr}(-\Delta H_r)]L/TD_{Se}C_{Ss}$	$\sigma$ controls the coupling between the chemical reaction velocity and mass flow	This cross-coefficient controls the mass flux induced by reaction, such as enzyme catalyzed reactions, growth of microorganisms utilizing single or multiple substrates. <sup>5,12,13</sup>
$\kappa = bC_{Ss}L\lambda_S/k_e T^2$	$\kappa$ controls the coupling between the chemical reaction velocity and heat flow	This cross-coefficient controls the heat flow induced by chemical reaction. For instance, anabolic pathways utilizes the energy generated during catabolism in order to produce various other metabolic molecules/compounds. <sup>5,6,20</sup>

utilization of  $\theta_S$  is high for higher values of cross-coefficient with time ( $z = 1$ ). The distribution of  $\theta_S$  for  $\tau = 1$  is similar for both low and high values of cross-coefficients until  $z = 0.9$ , where high values of cross-coefficients significantly changes  $\theta_S$  from 0.45 to 0.30. At  $z = \tau = 1$ , the remaining amount of  $\theta_S$  are 0.30 and 0.35 for high and low values of coefficients, respectively. The conversion rate and distribution analysis of  $\theta_S$  for both sets of value of cross-coefficients ( $\sigma = \kappa = \varepsilon = \omega = 0.0001$  and  $\sigma = \kappa = \varepsilon = \omega = 0.9$ ) shows that with increasing values of cross-coefficients, the substrate utilization advances (Figure 3a and c). The major effects of the cross-coefficients representing reaction-heat flow ( $\kappa$ ), reaction-mass flow ( $\sigma$ ), and heat-mass flows ( $\varepsilon$  and  $\omega$ ) can be observed in the temperature profile in time and space, as seen in Figure 3b and d. The high values of cross-coefficients results in rapid increase in temperature with time, whereas, in space, the temperature values remain constant until  $z \leq 0.9$ , and then rapidly increased until  $z = 1$ . The value of  $\phi$  increases from 1.00 to 1.12 with time (for  $z = 1$ ) for higher values of cross-coefficients, whereas remains almost constant for low values. The distribution of  $\phi$  with space ( $\tau = 1$ ) shows a shift from 1.00 to 1.10 at  $z = 0.9$ –1.0 for higher values of cross-coefficients, whereas the lower values, as similar to change in  $\phi$  with time, have a little change with space. Therefore, the change in  $\phi$  with both space and time increases significantly for high values of cross-coefficients ( $\sigma = \kappa = \varepsilon = \omega = 0.9$ ) than lower values ( $\sigma = \kappa = \varepsilon = \omega = 0.0001$ ). This indicates that the cross-coefficients play a significant role in terms of utilization of substrate and controlling temperature and hence, thermodynamic coupling could provide an insight in understanding reaction-transport processes in chemical and biochemical systems, such as the primary active transport, which requires the energy released by the hydrolysis of adenosine triphosphate in biological cells.<sup>5,12,27,28</sup>

**4.4. Biological Significance of Thermodynamic Coupling.** In order to characterize any biological system, the initial and boundary conditions considering subenvironmental resistances are imposed along with concentration of substrates and temperature. The effects of subenvironment resistances, bulk phase conditions, and cross-coefficients could easily

influence the efficiency of coupling.<sup>5</sup> Table 2 represents the related parameters used in this study with their respective definition and significance. These parameters have physical and biological meaning to the thermodynamically coupled reaction-transport processes. The change from a simple to a complex behavior is the order and coherence within a system that leads to coupled processes and organized dissipative structures. Turing represents the reaction-diffusion systems with appropriate nonlinear kinetics in a homogeneous steady state generating stable patterns.<sup>2</sup> The complexity of biochemical network systems is due to multiple interconnected branches and cycles, involving a number of coupled enzymatic processes. These enzymes sequentially convert different substrate with feedback and feed forward loop. For instance, primary active transport in biological cells involves hydrolysis of ATP coupled with the flows of sodium ions outside of the cell. In this case, ATP synthesis is matched and synchronized to cellular ATP utilization for the level of trans-membrane proton transport as well as other transport systems such as primary active transport of sodium–potassium pumps as shown in Figure 4. As a result, the hydrolysis of ATP is coupled to transporting protons, and maintaining the thermodynamic force of electrochemical ion gradients.<sup>9,12,14,23,26–28,31</sup> Consequently, these cross-coefficients

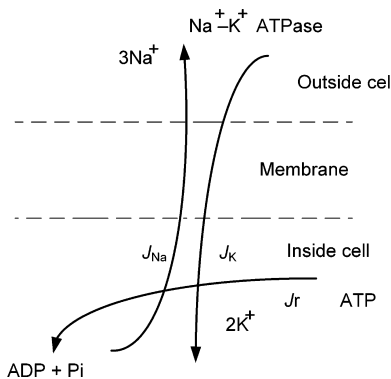


**Figure 4.** Primary active transport for  $\text{Na}^+$  and  $\text{K}^+$  pumps representing the thermodynamically coupled reaction-transport processes.

may also be useful in understanding of protein folding, biological oscillations, membrane transport, and various coupled biological phenomena. Modeling of biological systems requires quantitative predictions of the coupling and subenvironmental conditions representing the metabolic reaction-transport processes.<sup>9</sup>

The energy level of a reactant may change due to the coupling effect, while the catalyst effect may be limited to the lowering of the reaction barrier for both the forward and backward reactions.<sup>9</sup> Many biological reactions can take place against their own affinities because of the thermodynamic coupling effect. For example, many transport systems in bacteria are driven by the proton gradient across the plasma membrane. At the same time, protons are transported out of the cell in connection with electron flow through the respiratory chain. Overall, the cell maintains a nonequilibrium level of pH by keeping its interior at a higher pH than its environment. Eukaryotic cells possess a hierarchy of transport systems to maintain nonequilibrium concentration levels of some substrates within organelles than those in the cell's cytoplasm. Still, the cell controls its complex array of chemical reaction cycles so that the supply and demand for substrates, energy, and electrons are balanced and resources are utilized efficiently.<sup>3,9,19</sup>

Stucki<sup>26,31,32</sup> applied the linear nonequilibrium thermodynamics theory to oxidative phosphorylation within the practical range of phosphate potentials

$$X_p = -\Delta G_p^\circ - RT \ln \left( \frac{[ATP]}{[ADP][P_i]} \right) \quad (36)$$

A starting point in linear nonequilibrium thermodynamic formulations is the following representative dissipation function given by

$$T \frac{d_i S}{dt} = J_p A_p^{\text{ex}} + J_H \Delta \tilde{\mu}_H + J_O A_O^{\text{ex}} \quad (37)$$

Here, the subscripts P, H, and O refer to phosphorylation, the H<sup>+</sup> flow, and substrate oxidation, respectively, Δ̃μ<sub>H</sub> is the electrochemical potential difference of protons, and A<sup>ex</sup> is the external affinity. When the interior of the mitochondrion is in a stationary state, it suffices to measure the changes in the external solution only. From eq 37, the linear phenomenological equations with the resistance coefficients<sup>5,19</sup> are obtained

$$A_p^{\text{ex}} = K_p J_p + K_{PH} J_H + K_{PO} J_O \quad (38)$$

$$\Delta \tilde{\mu}_H = K_{HP} J_p + K_{HJ} J_H + K_{OH} J_O \quad (39)$$

$$A_O^{\text{ex}} = K_{OP} J_p + K_{HO} J_H + K_{OJ} J_O \quad (40)$$

With the rate of performance of electroosmotic work, we can define the effectiveness of energy conversion

$$\eta = -\frac{J_p X_p}{J_r A} \quad (41)$$

where X<sub>p</sub> is the force for proton transportation given in eq 40.<sup>3,5,9,19</sup>

**4.5. Special Reaction-Transport Cases.** When there is no coupling between the flow of hydrogen and ATP production, we have K<sub>PH</sub> = K<sub>HP</sub> = 0; using eqs 38 and 39 the phenomenological equations become

$$A_p^{\text{ex}} = K_p J_p + K_{PO} J_O \quad (42)$$

$$\Delta \tilde{\mu}_H = K_H J_H + K_{OH} J_O \quad (43)$$

Uncoupling proteins are a subgroup of the mitochondrial anion transporter family, and are identified in prokaryotes, plants, and animal cells. The uncoupling of the mitochondrial electron transport chain from the phosphorylation of ADP is physiological, optimizes the efficiency, and fine-tunes the degree of coupling of oxidative phosphorylation.<sup>19</sup>

When we have level flow, the force vanishes, Δ̃μ<sub>H</sub> = 0, and eqs 38 to 40 reduce to

$$A_p^{\text{ex}} = K_p (1 - q_{PH}^2) J_p - (K_p K_O)^{1/2} (q_{PO} + q_{PH} q_{OH}) J_O \quad (44)$$

$$A_O^{\text{ex}} = -(K_p K_O)^{1/2} (q_{PO} + q_{PH} q_{OH}) J_p + K_O (1 - q_{OH}^2) J_O \quad (45)$$

and the effective degree of coupling<sup>19,28</sup> becomes

$$q = \frac{q_{PO} + q_{PH} q_{OH}}{(1 - q_{PH}^2)(1 - q_{OH}^2)} \quad (46)$$

Using eqs 30–32, four cases of reaction-transport systems are analyzed.

**Case i.** No coupling between the flows of heat and mass involving Soret effect: ε = 0; the modeling equations become

$$\frac{\partial \theta_S}{\partial \tau} = \frac{\partial^2 \theta_S}{\partial z^2} + \frac{\sigma}{\phi^2} \frac{\partial \phi}{\partial z} - A^* D_{AS} \theta_{Seq} \exp \left[ \gamma_f \left( 1 - \frac{1}{\phi} \right) \right] \quad (47)$$

$$\begin{aligned} \frac{1}{Le} \frac{\partial \phi}{\partial \tau} &= \frac{\partial^2 \phi}{\partial z^2} + \omega \frac{\partial^2 \theta_S}{\partial z^2} - \frac{\kappa}{\phi} \frac{\partial \theta_S}{\partial z} + A^* D_{AS} \beta \theta_{Seq} \\ &\times \exp \left[ \gamma_f \left( 1 - \frac{1}{\phi} \right) \right] \end{aligned} \quad (48)$$

Equations 47, 48, and 32 are solved with respective parameters given in Table 1, and simulations are summarized in Figure S4 within the Supporting Information.

**Case ii.** No coupling between heat and mass flows involving Dufour effect: ω = 0; the modeling equations become

$$\begin{aligned} \frac{\partial \theta_S}{\partial \tau} &= \frac{\partial^2 \theta_S}{\partial z^2} + \varepsilon \frac{\partial^2 \phi}{\partial z^2} + \frac{\sigma}{\phi^2} \frac{\partial \phi}{\partial z} - A^* D_{AS} \theta_{Seq} \\ &\times \exp \left[ \gamma_f \left( 1 - \frac{1}{\phi} \right) \right] \end{aligned} \quad (49)$$

$$\begin{aligned} \frac{1}{Le} \frac{\partial \phi}{\partial \tau} &= \frac{\partial^2 \phi}{\partial z^2} - \frac{\kappa}{\phi} \frac{\partial \theta_S}{\partial z} + A^* D_{AS} \beta \theta_{Seq} \\ &\times \exp \left[ \gamma_f \left( 1 - \frac{1}{\phi} \right) \right] \end{aligned} \quad (50)$$

Equations 49, 50, and 32 are solved with respective parameters in Table 1, and simulations are summarized in Figure S5 within the Supporting Information.

**Case iii.** No coupling between the chemical reaction velocity and mass flow: σ = 0; the modeling equations become

$$\frac{\partial \theta_S}{\partial \tau} = \frac{\partial^2 \theta_S}{\partial z^2} + \varepsilon \frac{\partial^2 \phi}{\partial z^2} - A^* Da_S \theta_{Seq} \exp \left[ \gamma_f \left( 1 - \frac{1}{\phi} \right) \right] \quad (51)$$

$$\begin{aligned} \text{Le} \frac{1}{\partial \tau} \frac{\partial \phi}{\partial z} &= \frac{\partial^2 \phi}{\partial z^2} + \omega \frac{\partial^2 \theta_S}{\partial z^2} - \frac{\kappa}{\phi} \frac{\partial \theta_S}{\partial z} + A^* Da \beta \theta_{Seq} \\ &\times \exp \left[ \gamma_f \left( 1 - \frac{1}{\phi} \right) \right] \end{aligned} \quad (52)$$

Equations 51, 52, and 32 are solved with respective parameters in Table 1, and simulations are summarized in Figure S6 within the Supporting Information.

**Case iv.** No coupling between the chemical reaction velocity and heat flow:  $\kappa = 0$ ; the modeling equations become

$$\begin{aligned} \frac{\partial \theta_S}{\partial \tau} &= \frac{\partial^2 \theta_S}{\partial z^2} + \varepsilon \frac{\partial^2 \phi}{\partial z^2} + \frac{\sigma}{\phi^2} \frac{\partial \phi}{\partial z} - A^* Da_S \theta_{Seq} \\ &\times \exp \left[ \gamma_f \left( 1 - \frac{1}{\phi} \right) \right] \end{aligned} \quad (53)$$

$$\begin{aligned} \text{Le} \frac{1}{\partial \tau} \frac{\partial \phi}{\partial z} &= \frac{\partial^2 \phi}{\partial z^2} + \omega \frac{\partial^2 \theta_S}{\partial z^2} + A^* Da \beta \theta_{Seq} \\ &\times \exp \left[ \gamma_f \left( 1 - \frac{1}{\phi} \right) \right] \end{aligned} \quad (54)$$

Equations 53, 54, and 32 are solved with respective parameters in Table 1, and simulations are summarized in Figure S7 within the Supporting Information.

## 5. CONCLUSIONS

The modeling equations developed in the dimensionless and unidirectional forms are solved for a systematic study of the influences of external and internal factors on reaction-transport processes in space and time for an enzymatic conversion of a substrate to a product within the metabolic cycle. The external factors considered are the influences of subenvironment resistances to mass and heat flows as well as the bulk phase conditions, while the internal factors are the induced effects controlled by the unique cross-coefficients because of thermodynamic coupling between transport processes and enzymatic reaction. The representative solutions display the effect of each influence on the substrate concentration and temperature in both time and space when the other possible influences are kept the same. However, the complex coupled biochemical cycles will be affected by all types of these influences simultaneously. Yet, the comprehensive modeling presented in this study may provide a thorough analysis tool for understanding the effects of subenvironmental conditions and induced effects because of thermodynamic coupling on the reaction-transport processes in chemical and biochemical systems when they are in the vicinity of equilibrium.

## ■ ASSOCIATED CONTENT

### Supporting Information

SA: Two-dimensional plots for changes in  $\theta_S$  and  $\phi$  with space (at  $\tau = 1$ ) and time (at  $z = 1$ ) using the parameters in Table S1 are given in Figures S1, S2, and S3. SB: Special reaction transport cases: (i) no coupling between the flows of heat and mass involving Soret effect (Figure S4), (ii) no coupling between heat and mass flows involving Dufour effect (Figure

S5), (iii) no coupling between the chemical reaction velocity and mass flow (Figure S6), and (iv) no coupling between the chemical reaction velocity and heat flow (Figure S7). This material is available free of charge via the Internet at <http://pubs.acs.org/>.

## ■ AUTHOR INFORMATION

### Corresponding Author

\*Tel.: +1-402-472-2750. E-mail: rahultevatia\_83@yahoo.co.in.

### Notes

The authors declare no competing financial interest.

## ■ NOMENCLATURE

A	chemical affinity, J/mol
Da	Damköhler number
$D_S$	effective diffusion coefficient for the substrate S, m <sup>2</sup> /s
$D_D$	coupling coefficient related to the Dufour effect, J m <sup>2</sup> /(mol s)
$D_T$	coupling coefficient related to the thermal diffusion (Soret) effect, mol/(m s K)
E	activation energy of the chemical reaction, J/mol
$\Delta H_r$	reaction enthalpy J/kg
h	heat transfer coefficient, J/(m <sup>2</sup> K)
$H_i$	partial enthalpy, J/kg
J	diffusive molar flux, mol/(m <sup>2</sup> s)
$J_q$	conduction heat flux, W/m <sup>2</sup>
$J_r$	volumetric reaction rate, mol/(m <sup>3</sup> s)
k	effective thermal conductivity, W/(m K)
Le	Lewis number
$L_{ik}$	phenomenological coefficients
$L_{qr}$	element of coupling coefficient between chemical reaction and heat flow, mol K/(m <sup>2</sup> s)
$L_{ir}$	element of coupling coefficient between chemical reaction and mass flow of component i, mol <sup>2</sup> K/(J m <sup>2</sup> s)
Nu	Nusselt number (Nu = $hL/k$ )
R	gas constant, J/(mol K)
S	entropy, J/(mol K)
Sh	Sherwood number (Sh <sub>i</sub> = $k_g L/D_i$ )
t	time, s
T	temperature, K
z	dimensionless distance

### Greek Letters

$\beta$	thermicity group, dimensionless
$\varepsilon$	dimensionless parameter related to Soret effect
$\gamma$	Arrhenius group, dimensionless
$\phi$	dimensionless temperature
$\mu$	chemical potential, J/mol
$\theta$	dimensionless composition
$\nu$	stoichiometric coefficient
$\rho$	density, kg/m <sup>3</sup>
$\tau$	dimensionless time
$\omega$	dimensionless parameter related to Dufour effect

### Subscripts

b	bulk phase
D	Dufour
e	effective
eq	equilibrium
P	product
q	heat
r	reaction
s	surface
T	thermal diffusion

S component S

## ■ REFERENCES

- (1) Davies, P. C. W.; Rieper, E.; Tuszyński, J. A. Self-organization and entropy reduction in a living cell. *BioSystems* **2013**, *111*, 1–10.
- (2) Virgo, N.; Law, R.; Emmerson, M. Sequentially assembled food webs and extremum principles in ecosystem ecology. *J. Anim. Ecol.* **2006**, *75*, 377–386.
- (3) Vershubskii, A. V.; Priklonskii, V. I.; Tikhonov, A. N. Effects of diffusion and topological factors on the efficiency of energy coupling in chloroplast with heterogeneous partitioning of protein complexes in thylakoids of grana and stroma. A mathematical model. *Biochem. (Mosc)* **2004**, *69*, 1016–1024.
- (4) Ji, L.; Li, Q. S. Turing pattern formation in coupled reaction-diffusion systems: Effect of subenvironment and external influence. *Chem. Phys. Lett.* **2006**, *424*, 432–436.
- (5) Demirel, Y. *Non-equilibrium Thermodynamics: Transport and Rate Processes in Physical, Chemical and Biological Systems*; 3rd ed.; Elsevier: Amsterdam, 2014.
- (6) Demirel, Y.; Sandler, S. I. Linear-nonequilibrium thermodynamics theory for coupled heat and mass transport. *Int. J. Heat Mass Transfer* **2001**, *44*, 2439–2451.
- (7) Turing, A. M. The chemical basis of morphogenesis. *Philos. Trans. R. Soc. London B* **1952**, *237*, 37–72.
- (8) Demirel, Y. Modeling of thermodynamically coupled reaction-transport systems. *Chem. Eng. J.* **2008**, *139*, 106–117.
- (9) Demirel, Y.; Sandler, S. I. Thermodynamics and bioenergetics. *Biophys. Chem.* **2002**, *97*, 87–111.
- (10) Tevaticia, R.; Demirel, Y.; Blum, P. Kinetic modeling of photoautotrophic growth and neutral lipid accumulation in terms of ammonium concentration in *Chlamydomonas reinhardtii*. *Bioresour. Technol.* **2012**, *119*, 419–424.
- (11) Demirel, Y. Nonequilibrium thermodynamics modeling of coupled biochemical cycles in living cells. *J. Non-Newtonian Fluid Mech.* **2010**, *165*, 953–972.
- (12) Nath, S. A thermodynamic principle for the coupled bioenergetic processes of ATP synthesis. *Pure Appl. Chem.* **1998**, *70*, 639–644.
- (13) Chowdhury, S.; Chanda, B. Thermodynamics of electro-mechanical coupling in voltage-gated ion channels. *J. Gen. Physiol.* **2012**, *140*, 613–623.
- (14) Murugan, R. Theory on thermodynamic coupling of site-specific DNA–protein interactions with fluctuations in DNA-binding domains. *J. Phys. A: Math. Theor.* **2011**, *44*, 505002–505014.
- (15) Zharov, V. P.; Latyshev, A. S. Laser ultrasonic transport of drugs in living tissues. *Ann. N.Y. Acad. Sci.* **1998**, *858*, 66–73.
- (16) Mayorga, L. S.; Lopez, M. J.; Becker, W. M. Molecular thermodynamics for cell biology as taught with boxes. *CBE Life. Sci. Educ.* **2012**, *11*, 31–38.
- (17) Popov, E. M. Protein folding as a nonlinear nonequilibrium thermodynamic process. *Biochem. Mol. Biol. Int.* **1999**, *47*, 443–453.
- (18) Wassenaar, R. H.; Westra, J. J. W. Dynamic model of a film absorber with coupled heat and mass transfer. *Int. J. Heat Mass Transfer* **1992**, *35*, 87–99.
- (19) Caplan, S. R.; Essig, A. *Bioenergetics and Linear Nonequilibrium Thermodynamics: The Steady State*; Harvard University Press: Cambridge, MA, 1999.
- (20) Cortassa, S.; Aon, M. A.; Westerhoff, H. V. Linear non-equilibrium thermodynamics describes the dynamics of an autocatalytic system. *Biophys. J.* **1991**, *60*, 794–803.
- (21) Rothschild, K. J.; Ellias, S. A.; Essig, A.; Stanley, H. E. Nonequilibrium linear behavior of biological systems. Existence of enzyme-mediated multidimensional inflection points. *Biophys. J.* **1980**, *30*, 209–230.
- (22) Demirel, Y.; Sandler, S. I. Nonequilibrium thermodynamics in engineering and science. *J. Phys. Chem. B* **2004**, *108*, 31–43.
- (23) Cukrowski, A. S.; Kolbus, A. On validity of linear phenomenological nonequilibrium thermodynamics equations in chemical kinetics. *Acta Phys. Polym., B* **2005**, *36*, 1485–1507.
- (24) Froment, G. F.; Bischoff, K. B.; De Wilde, J. *Chemical Reactor Analysis and Design*; 3rd ed.; Wiley, 2010.
- (25) Borghini, N. *Topics in Nonequilibrium Thermodynamics*; University Bielefeld: Bielefeld, Germany, 2014; <http://www.physik.uni-bielefeld.de/~borghini/Teaching/Nonequilibrium/Nonequilibrium.pdf>.
- (26) Stucki, J. W. The optimal efficiency and the economic degrees of coupling of oxidative phosphorylation. *Eur. J. Biochem.* **1980**, *109*, 269–283.
- (27) Jin, Q.; Bethke, C. M. Kinetics of electron transfer through the respiratory chain. *Biophys. J.* **2002**, *83*, 1797–1808.
- (28) Kedem, O.; Caplan, S. R. Degree of coupling and its relation to efficiency in energy conversion. *Trans. Faraday Soc.* **1965**, *61*, 1897–1911.
- (29) Jiao, A.; Zhang, Y.; Ma, H.; Critser, J. Effects of Lewis number on coupled heat and mass transfer in a circular tube subjected to external convective heating. *J. Heat Transfer* **2009**, *131*, 591–598.
- (30) Huang, M. J.; Kapral, R.; Mikhailov, A. S.; Chen, H. Y. Coarse-grain simulations of active molecular machines in lipid bilayers. *J. Chem. Phys.* **2013**, *138*, 195101–11.
- (31) Qian, H. Phosphorylation energy hypothesis: Open chemical systems and their biological functions. *Annu. Rev. Phys. Chem.* **2007**, *58*, 113–142.
- (32) Stucki, J. W. Non-equilibrium thermodynamic sensitivity of oxidative phosphorylation. *Proc. Biol. Sci.* **1991**, *244*, 197–202.